NAVAL POSTGRADUATE SCHOOL

MONTEREY, CALIFORNIA

THESIS

METALLOID ALUMINUM CLUSTERS WITH FLUORINE

by

Nape D. Lentsoane

December 2016

Thesis Advisor: Joseph Hooper
Second Reader: James Luscombe

THIS PAGE INTENTIONALLY LEFT BLANK

REPORT DOCUMENTATION PAGE			Form Approved OMB No. 0704-0188

1. AGENCY USE ONLY *(Leave blank)*	2. REPORT DATE	3. REPORT TYPE AND DATES COVERED
	December 2016	Master's thesis

4. TITLE AND SUBTITLE
METALLOID ALUMINUM CLUSTERS WITH FLUORINE

5. FUNDING NUMBERS

6. AUTHOR(S) Nape D. Lentsoane

7. PERFORMING ORGANIZATION NAME(S) AND ADDRESS(ES)
Naval Postgraduate School
Monterey, CA 93943-5000

8. PERFORMING ORGANIZATION REPORT NUMBER

9. SPONSORING /MONITORING AGENCY NAME(S) AND ADDRESS(ES)
N/A

10. SPONSORING / MONITORING AGENCY REPORT NUMBER

11. SUPPLEMENTARY NOTES The views expressed in this thesis are those of the author and do not reflect the official policy or position of the Department of Defense or the U.S. Government. IRB number ____N/A____.

12a. DISTRIBUTION / AVAILABILITY STATEMENT
Approved for public release. Distribution is unlimited.

12b. DISTRIBUTION CODE

13. ABSTRACT (maximum 200 words)

Metals have a very high energy density compared to explosives, but typically release this energy slowly via diffusion-limited combustion. There is recent interest in using molecular-scale metalloid clusters as a way to achieve very rapid rates of metal combustion. These clusters contain a mixture of low-valence metals as well as organic ligands. Here we investigate a prototypical aluminum metalloid cluster to determine system stability if the organic ligand contains significant amounts of fluorine. The fluorine can, in principle, oxidize the metallic elements, resulting in a system much like organic explosives where the fuel and oxidizer components are mere angstroms apart. We performed density functional theory calculations within the SIESTA code to examine the cluster binding energy and electronic structure. Partial fluorine substitution in a prototypical aluminum-cyclopentadienyl cluster results in increased binding and stability, likely due to weak non-covalent interactions between ligands. Ab initio molecular dynamics simulations confirm that the cluster is structurally stable when subjected to simulated annealing at elevated temperatures.

14. SUBJECT TERMS	15. NUMBER OF PAGES
density functional theory, molecular dynamics, binding energy, siesta code, density of states, projected density of states	69
	16. PRICE CODE

17. SECURITY CLASSIFICATION OF REPORT	18. SECURITY CLASSIFICATION OF THIS PAGE	19. SECURITY CLASSIFICATION OF ABSTRACT	20. LIMITATION OF ABSTRACT
Unclassified	Unclassified	Unclassified	UU

NSN 7540-01-280-5500 Standard Form 298 (Rev. 2-89)
Prescribed by ANSI Std. 239-18

THIS PAGE INTENTIONALLY LEFT BLANK

Approved for public release. Distribution is unlimited.

METALLOID ALUMINUM CLUSTERS WITH FLUORINE

Nape D. Lentsoane
Civilian, Armaments Corporation of South Africa (Armscor)
M.Tech., Tshwane University of Technology, 2008

Submitted in partial fulfillment of the
requirements for the degree of

MASTER OF SCIENCE IN APPLIED PHYSICS

from the

NAVAL POSTGRADUATE SCHOOL
December 2016

Approved by: Joseph Hooper
Thesis Advisor

James Luscombe
Second Reader

Kevin Smith
Chair, Department of Physics

THIS PAGE INTENTIONALLY LEFT BLANK

ABSTRACT

Metals have a very high energy density compared to explosives, but typically release this energy slowly via diffusion-limited combustion. There is recent interest in using molecular-scale metalloid clusters as a way to achieve very rapid rates of metal combustion. These clusters contain a mixture of low-valence metals as well as organic ligands. Here we investigate a prototypical aluminum metalloid cluster to determine system stability if the organic ligand contains significant amounts of fluorine. The fluorine can, in principle, oxidize the metallic elements, resulting in a system much like organic explosives where the fuel and oxidizer components are mere angstroms apart. We performed density functional theory calculations within the SIESTA code to examine the cluster binding energy and electronic structure. Partial fluorine substitution in a prototypical aluminum-cyclopentadienyl cluster results in increased binding and stability, likely due to weak non-covalent interactions between ligands. Ab initio molecular dynamics simulations confirm that the cluster is structurally stable when subjected to simulated annealing at elevated temperatures.

THIS PAGE INTENTIONALLY LEFT BLANK

TABLE OF CONTENTS

THIS PAGE INTENTIONALLY LEFT BLANK

LIST OF FIGURES

LIST OF TABLES

THIS PAGE INTENTIONALLY LEFT BLANK

LIST OF ACRONYMS AND ABBREVIATIONS

CG	Conjugate Gradient
Cp	Cyclopentadienyl
DFT	Density Functional Theory
DOS	Density of States
fs	femto-second
GGA	Generalized Gradient Approximation
H-K	Hohenberg-Kohn theorem
HPC	High Performance Computing
K-S	Kohn-Shame framework
LDA	Local Density Approximation
MD	Molecular Dynamics
NVE	Constant number, Volume, and Energy
NVT	Constant number, Volume, and Temperature
Ry	Rydberg

THIS PAGE INTENTIONALLY LEFT BLANK

ACKNOWLEDGMENTS

I would like to express my gratitude to my advisor and second reader for their continued support. I would like to acknowledge my family for their support and patience.

I dedicate this work to Abbaasah and my two kids, Samira and Nusaybah.

THIS PAGE INTENTIONALLY LEFT BLANK

I. INTRODUCTION AND LITERATURE REVIEW

Metals are highly energetic materials that are commonly used to enhance explosive formulations. Despite their high energy content, metals tend to burn slowly through a diffusion-limited process. Recently there has been interest in creating low-valence metal clusters which retain some of the high energy density of bulk metals but may allow for significantly faster combustion kinetics. The core of this research work is to study hypothetic fluorinated aluminium clusters to determine their electronic structure and stability. The fluorine is integrated directly into the ligands around the cluster, placing low-valence metal fuel within a few chemical bonds of a strong oxidizer. Density functional theory as implemented in the SIESTA code is used to study these systems, and ab initio molecular dynamics is used as an initial check on their stability.

A number of previous works have examined aluminium-based clusters. Mandado et al. [1] studied the properties of bonding in all-metal clusters containing Al_4 units. The Al_4 was evaluated when attached to an alkaline or transitional metals, namely Na, Li, Be, Cu and Zn. Mandado et al. [1] employed Density Functional Theory (DFT) methods combined with the quantum theory of atoms in molecules (QTAIM) to study the local aromaticity of Al_4 fragments.

Various aluminium type clusters were evaluated by Williams and Hooper [2]. Williams and Hooper focused their study on the structure, thermodynamics and energies of Aluminium-Cyclopentadienyl clusters [2]. The study used the B3LYP functional performed with the Gaussian 09 program and compared to the G2 method. The clusters were of types Al_4Cp_4, Al_4Cp_4*, Al_8Cp_4, Al_8Cp_4*, $Al_{50}Cp_{12}$, and $Al_{50}Cp_{12}$*. The Cp derivatives were nitro-Cp ($C_5H_4NO_2$), trifluoromethyl-Cp* ($C_5Me_4CF_3$), and pentatrifluoromethyl-Cp* ($C_5[CF_3]_5$) which served as oxidizers for the aluminium complexes [2]. Williams and Hooper found that $AlCp_3$ and $AlCp_3$* systems exhibited significant steric interaction between the ligands [2]. In conclusion, Williams and Hooper suggested that thermal decomposition in these clusters will proceed via the loss of surface metal ligand

units, exposing the interior aluminium core. The energy density of the large clusters, as gauged by their volumetric heat of combustion, was calculated to be nearly 60% that of pure aluminium [2].

In this work, we examine clusters that contain a combination of metal-metal Al bonds as well as metal/organic bonds. These are often given the term “metalloid” and were investigated extensively by Schnockel and collaborators [3]. We focus on a small, prototypical cluster containing four aluminium atoms, each attached to a cyclopentadienyl (Cp) type ligand. Our particular focus is on integration of fluorine into these ligands. Fluorine is attractive because it can serve as a powerful oxidizer for the low-valent aluminium core in these clusters, and its close proximity in the cluster may avoid lengthy mass diffusion processes for fuel and oxidizer to mix. We evaluate the stability, binding energy, and electronic structure of Cp-type ligands with either one or five methyl groups replaced with trifluoromethyl (-CF_3) groups.

For our study the focus has been restricted to analyzing the fluorinated and non-fluorinated monomers (AlCp*) $AlC_{10}H_{12}F_3$, $AlC_{10}F_{15}$, and $AlC_{10}H_{15}$ and the fluorinated and non-fluorinated clusters (Al_4Cp_4*) $Al_4C_{40}F_{60}$, $Al_4C_{40}H_{48}F_{12}$, $Al_4C_{40}H_{60}$. The binding energy of the tetramers is then compared to that of the basic single aluminium with ligand molecules. For all systems geometric optimization is performed. Our Molecular dynamics is focused on the partially-fluorinated ($Al_4C_{40}H_{48}F_{12}$) and the fully-hydrogenated ($Al_4C_{40}H_{60}$) clusters. The fully-hydrogenated cluster has already been well characterized experimentally by Huber and Schnöckel [3].

Wantanabe et al. [4] used DFT to study the stabilization of an Al_{13} cluster with Poly(vinylpyrrolidone) (PVP). Wantanabe et al. [4] found that stabilization was mainly due to bonding interactions between molecular orbitals of PVP and the 1s or 1d orbitals of Al_{13}. A study involving the binding of Aluminium to Fluorine was undertaken by Karpukhina et al. [5]. The systems were of alkali-fluoride types. The targeted application was heat-resistant glass ceramic. It was found that for aluminosilicate glasses the Al-F bonding increases with

temperature. The reactivity of the H atom with Al13 cluster was also analyzed by Mañanes et al. [6]. Although density functional concepts were used, Mañanes et al. also employed Fukui analysis.

All calculations in this work are performed with the SIESTA code. SIESTA scales very efficiently with the number of atoms and with parallel processing power, making it a suitable choice for eventual simulations of metalloid clusters with thousands of atoms [7]. The code uses the standard Kohn-Sham self-consistent density functional method in the local density (LDA-LSD) and generalized gradient (GGA) approximations, as well as in a non-local functional that includes van der Waals interactions (VDW-DF) [8]. SIESTA uses norm-conserving pseudopotentials that are available online from the SIESTA website. In this work we used default pseudopotential from the SIESTA repository at http://departments.icmab.es/leem/siesta/Databases.

The chapter outline of this report is as follows. In Chapter I current available literature is reviewed and scope of this report given. In Chapter II the purpose of our study is concisely defined. Chapter III presents density functional theory, and the theory behind molecular dynamics. The Monte-Carlo runs computed with SIESTA for molecular dynamics are performed with the Nose method (NVT dynamics with Nose thermostat). In Chapter IV is the simulation setup. Results and analysis follow in Chapter V and concluding remarks in Chapter VI.

THIS PAGE INTENTIONALLY LEFT BLANK

II. PROBLEM DEFINITION

The purpose of this thesis is to understand the aluminium based monomers and Al_4 clusters, including their stability geometry, and electronic structure. The binding energy will be analyzed as well as the interaction between the molecular orbitals and thus which orbitals are responsible for the binding. Structural relaxation will be performed and final energy of the system computed.

The secondary goal is to simulate the molecular dynamics of the system and evaluate how the system evolves with time. This is also a simple way to roughly examine the influence of temperature on the systems. In Molecular Dynamics simulations, one computes the evolution of the positions and velocities with time, solving Newton's equations. The SIESTA code contains the algorithms to perform this. The Nose (NVT dynamics with Nose thermostat) method is used to perform molecular dynamics.

The research question explored in this paper is: Are metalloid aluminum clusters using fluorinated Cp ligands just as stable as those with traditional Cp?

THIS PAGE INTENTIONALLY LEFT BLANK

III. THEORY

A. DENSITY FUNCTIONAL THEORY

Density functional theory has been in use for many years. The DFT is used to study the electronic structure of many-body systems [9]. The many-body systems investigated include atoms, molecules, and condensed phases [9]. In principle the idea is to find the ground state of these systems. The DFT roots can be traced as far back as the mid-1960s in the Hohenberg–Kohn theorems (H-K). Functional simply refers to the function of a function. The challenge in this quantum mechanical modeling method is then to find the correct ground state of electron density that achieves energy minimization. The SIESTA code used in this study employs the framework of Kohn-Sham DFT.

Fundamentally in DFT we solve the many-body Schrödinger equation:

$$\widehat{H}\psi\left(\{r_i\},\{R_I\}\right)=E\psi\left(\{r_i\},\{R_I\}\right),$$

where $\widehat{H}$ is the Hamiltonian operator, r_i and R_I are a bunch of electrons and nuclei respectively, and E is the total energy. The Hamiltonian operator is an energy operator defined as

$$\widehat{H}=\widehat{T}+\widehat{V}_{coulomb}$$

Here, $\widehat{T}$ is the kinetic energy operator, and $\widehat{V}_{coulomb}$ is the coulomb potential operator also defined as

$$\widehat{V}_{coulomb}=\frac{q_i q_j}{\left|\vec{r_i}-\vec{r_j}\right|}$$

The $\widehat{V}_{coulomb}$ operator describes the interaction between charged particles. The above equation involves a bunch of electrons and a bunch of nuclei which makes solving it more complex. To remedy the complexity, the Born

Oppenheimer approximation is used. The Born Oppenheimer approximation states that the mass of the nuclei is much greater than that of the electrons i.e. $m_{nuclei} \gg m_e$ [10]. Also the nuclei are slow whilst the electrons are fast. This implies that we can decouple the dynamics of the nuclei and the electrons.

$$\Rightarrow \quad \psi\left(\{r_i\},\{R_I\}\right) \rightarrow \psi_N\left(\{r_i\}\right) * \psi_e\left(\{R_I\}\right)$$

This reduces the number of variables in the original equation to focus on a finite number of electrons.

$$\widehat{H}\psi(\mathbf{r}_1,\mathbf{r}_2,...,\mathbf{r}_N) = E\psi(\mathbf{r}_1,\mathbf{r}_2,...,\mathbf{r}_N)$$

The Hamiltonian will now consist of terms dealing with electrons only,

$$\widehat{H} = -\frac{h^2}{2m_e}\sum_i^{N_e}\nabla_i^2 + \sum_i^{N_e}V_{ext}(r_i) + \sum_i^{N_e}\sum_{j>1}U(r_i,r_j)$$

The second term in the above equation is the potential term that encompasses the electron-nuclei interaction. The last term is the electron-electron interaction (i.e., repulsions). Even though the equations have been reduced to electron terms the challenge is still to reduce the dimensionality. To state the problem of dimensionality, for example, Al has 13 electrons and each electron is defined by three spatial coordinates. Therefore the solving the Schrödinger equation becomes a 39 dimensional problem ($3\times13=39$) for a single Al atom. Thus when forming a cluster the dimensions increase in multiples e.g., 50 Al atoms in a cluster implies 1950 dimensional problem and a 100 atom Au cluster is a 23700 dimensional problem.

The DFT deals with the dimensionality problem by defining the electron density

$$n(\mathbf{r}) = \psi^*(\mathbf{r}_1,\mathbf{r}_2,...\mathbf{r}_N)\psi(\mathbf{r}_1,\mathbf{r}_2,...\mathbf{r}_N)$$

or, more compactly,

$$n(\mathbf{r}) = 2\sum_i \psi_i^*(\mathbf{r})\psi_i(\mathbf{r})$$

and therefore the dimensionality goes as $3N \to 3$. This changes the problem to a many one electron problem. Recall that from the H-K theorem we are trying to find the ground state energy E. The ground state energy is said to be a unique functional [10].

$$E = E[n(\mathbf{r})]$$

To find the ground state the energy functional is minimized by searching for a zero gradient along the energy surface. The energy functional consists of two parts. The part that is known involves the kinetic energy and all the potentials aforementioned. The unknown part, exchange-correlation functional, has to be approximated. Available in SIESTA are the Local Density Approximation (LDA) and the Generalized Gradient Approximation (GGA). For our work we use the GGA. In obtaining the true ground state SIESTA employs the Kohn-Sham self-consistency scheme. The self-consistency scheme's first step is to arbitrarily guess the input electron density $n(\mathbf{r})$. Thereafter solve the Kohn-Sham equations to find a set of electron wave functions ψ_i. Re-use these wave functions to calculate the electron density. The calculated electron density is then matched with the input electron density. If the calculated and the input are the same then the ground state has been found otherwise repeat the process. In SIESTA the tolerance of this sameness can be specified.

Molecular geometry optimization. In investigating our chosen systems we perform geometry optimization of the molecules as a first step. Geometry optimization is a process of searching for the coordinates that minimize the total energy of the system. The search can be stated mathematically as

$$\{x_i, y_i, z_i\}_{t=0} = \arg\min_{x_i, y_i, z_i}\left(\left\langle \Psi \middle| \widehat{H} \middle| \Psi \right\rangle\right)$$

where x_i, y_i, z_i are the spatial positions of the atoms. Once again we look for zero gradient of the energy

$$(\nabla E)_i = \frac{\partial E}{\partial \vec{x}_i}$$

Our SIESTA setup uses the conjugate gradient (CG). The CG is used to solve the unconstrained optimization problem. The ways to verify if SIESTA has performed the structural geometry relaxation correctly are discussed in Chapter V (Results and Analysis). SIESTA will also churn out the atomic forces at every relaxation step as it attempts to find the ground state.

The pseudopotential files, required at runtime, characterize the electron density with a smoothed density. This is referred to as the frozen core approximation [10].

B. MOLECULAR DYNAMICS

Generally, in molecular dynamics we are attempting to solve Newton's 2nd law for our molecular system(s). Molecular dynamics (MD) treats electrons quantum mechanically and nuclei classically [11]. In MD we are able to investigate the time evolution of the system. MD also allows us to evaluate the influence of temperature on the molecular system. Thus, we gain information about the thermal stability of our clusters.

The basic equation to be solved in MD is

$$\vec{F}(t) = -\frac{dE}{d\vec{x}} = m\vec{a}(t) = m\frac{d^2\vec{x}(t)}{dt^2}$$

$$\Rightarrow \quad \vec{x}(t) = \vec{x}(t_0) + \vec{v}(t_0)(t - t_0) + \int_{t_0}^{t} dt' \int_{t_0}^{t} \frac{1}{m} \vec{F}(t'')dt''$$

The MD simulation computes the system evolution of positions and velocities with time [11]. The simulation obtains positions and velocities at a later time $t + \Delta t$. The SIESTA simulation setup allows the user to choose Δt referred to as the time step. In our simulations we set time step to 1 fs (femto-second). A smaller Δt improves the accuracy of sampling high frequency motion. The equations of motion are solved at each time step. MD continually takes the time averages and statistical averages until the system reaches equilibrium. The system is at equilibrium if the averages of the dynamical and structural quantities remain unchanged with time.

There are various algorithms available for MD in SIESTA. For our setup we used both the NVE (Verlet) and NVT (Nose). The Verlet employs a microcanonical ensemble, whereby the total energy is kept constant. Therefore, the Verlet is used to verify for correct parameterization by checking for energy conservation violations. In the Nose (canonical ensemble) case the enforced temperature is kept constant while changing the kinetic energy of the atoms.

THIS PAGE INTENTIONALLY LEFT BLANK

IV. SIMULATION SETUP

The simulation process is simplified as having four basic attributes: the input, simulation block, post-processing, and output. The simulation block is where all the SIESTA algorithms are located i.e. geometry optimization and MD. This process is depicted in Figure 1.

Figure 1. The simulation process

The simulation is performed with resources from Hamming HPC. In order for the SIESTA jobs to run parallel on Hamming we require the Intel compiler, OpenMPI and a compiled version of SIESTA. These packages are version sensitive and therefore care must be ensured when working with them. A simple script based on SLURM was written to schedule the jobs on Hamming. The SLURM script tells Hamming where to find the Intel compiler, OpenMPI and SIETA executables. Also, the SLURM script specifies required memory, number of nodes and wall time. The code snippet in Appendix B illustrates the SLURM script.

In the snippet in Appendix B, one node with 64 tasks per node is requested from Hamming. The memory required is 1 Gigabyte. The wall time is set at 72 hours, which is reasonable because although the optimization takes approximately 4 to 5 hours, the MD runs normally take 3 days or more. The Intel compiler version 17.0 and OpenMPI version 2.0.1 were found to work well with the SIESTA version 3.2-pl-5. Other versions are available but gave compatibility errors. The output is redirected to the '*.out' file.

For SIESTA to run correctly the input must be in the correct format. The main input file that tells SIESTA what to do is in the Flexible Data Format (FDF)

with the extension '*.fdf'. As an example, the FDF file for the $AlC_{10}H_{12}F_3$ system is attached in Appendix A. A thorough description of the FDF file can be found in the SIESTA manual [7]. Here we describe some of the important parameters of our setup.

The total number of atoms in a molecule is specified. The number of atom species contained in the molecule is also given as an input. For example, the $AlC_{10}H_{12}F_3$ has four number of atoms species. SIESTA will match the values of these parameters with the number of positions it finds in the supplied spatial coordinates. The coordinates are specified in angstroms.

The exchange-correlation functional is set to Generalized Gradient Approximation (GGA, PBE version) for all systems. The basis size is set to Double Zeta with Polarization (DZP). When performing structural relaxation, the Conjugate Gradient (CG) minimization algorithm is used. The other important parameter goes about how best to mesh the electron density. The mesh size, also called the mesh cut-off energy, is chosen to be 360 Ry (Rydberg). To find the optimal cut-off energy we compute the single point energy calculation. The calculation is performed with different mesh sizes. The mesh size is tweaked until the computed energy changes only by small amounts. We then plot the final energy vs mesh to evaluate the energy profiles of the systems. Figure 2 shows the energy profile for finding the optimal mesh cut-off. The final energy continues to descend until it no longer has significant changes. As can be seen in the figure the final energy difference between 350 Ry and 360 Ry is approximately 0.1 meV. Beyond this point the energy does not change significantly and therefore 360 Ry was chosen as the optimal mesh cut-off energy.

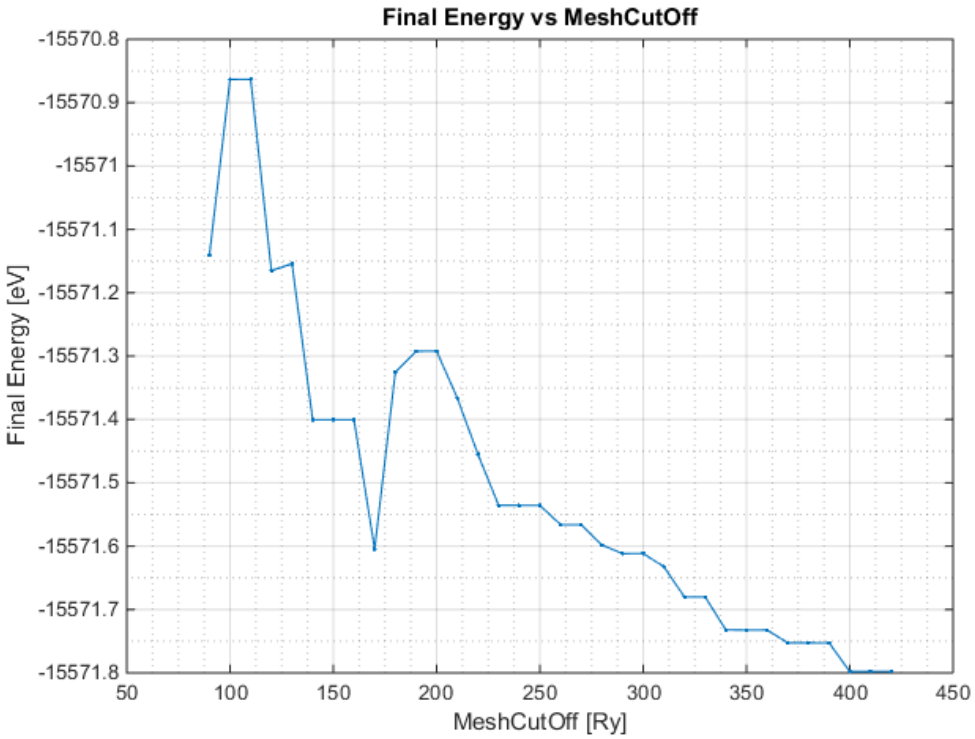

Figure 2. Single point energy profile vs. mesh cut-off. Optimal mesh cut-off found at 360 Ry.

Once the mesh cut-off energy has been found we are ready to perform geometry optimization. The number of CG steps maximally allowed is 500. The tolerance in the computed forces is set to 0.04 eV/Ang. The simulation box size remains default. The rest of the FDF file specifies which output to write out.

The MD scheme we are mostly interested in is the NVT Nose canonical ensemble. The NVE (Verlet) is also used but rather mainly for ensuring that energy is properly conserved with the chosen parameters. Also, the Verlet algorithm helps in finding the best parameter specification for the Nose. The optimal length of a time step was found to be 0.5 fs (femto-second). The MD runs are all performed with a temperature of 600K enforced.

The systems under investigation. The systems we investigated are 3 monomers ($AlC_{10}H_{12}F_3$, $AlC_{10}F_{15}$, and $AlC_{10}H_{15}$) and 3 tetramers ($Al_4C_{40}F_{60}$,

$Al_4C_{40}H_{48}F_{12}$, and $Al_4C_{40}H_{60}$). These systems are shown in Figure 3 through Figure 8.

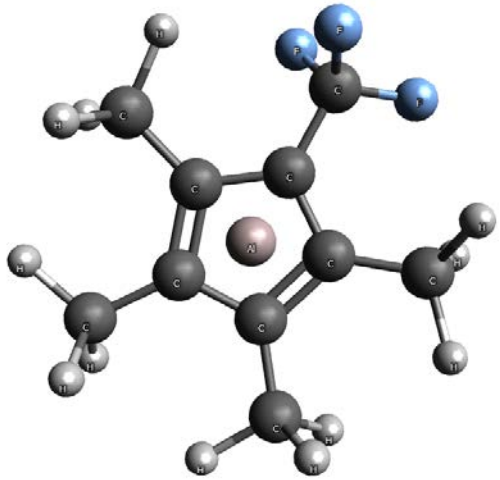

Figure 3. Monomer $AlC_{10}H_{12}F_3$

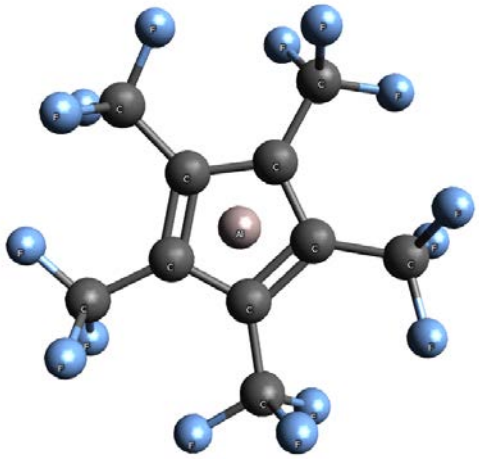

Figure 4. Monomer $AlC_{10}F_{15}$

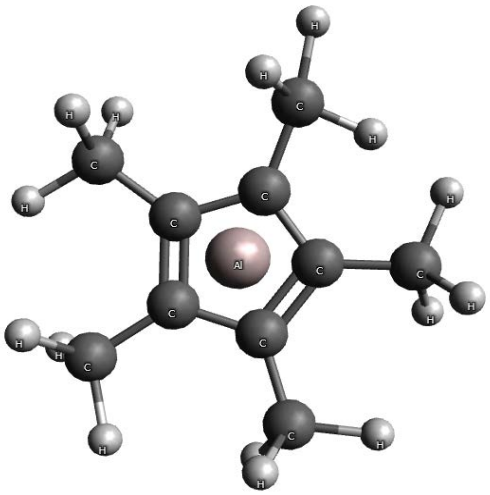

Figure 5. Monomer $AlC_{10}H_{15}$

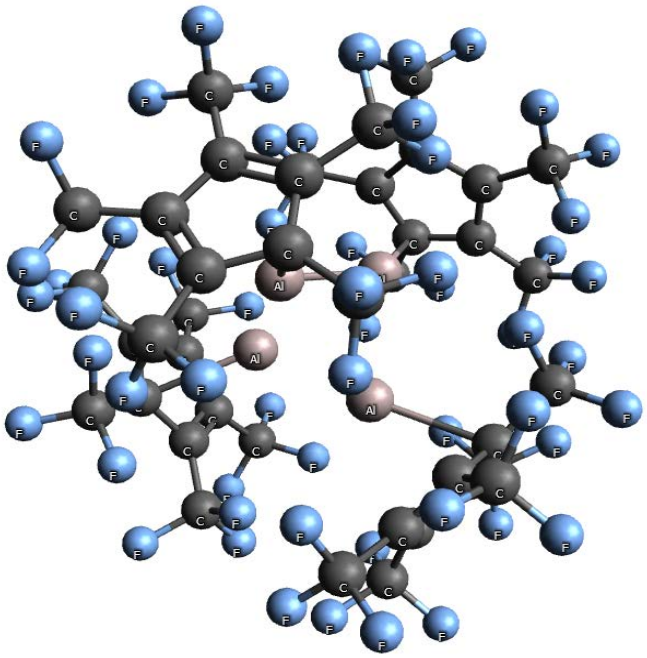

Figure 6. Tetramer $Al_4C_{40}F_{60}$

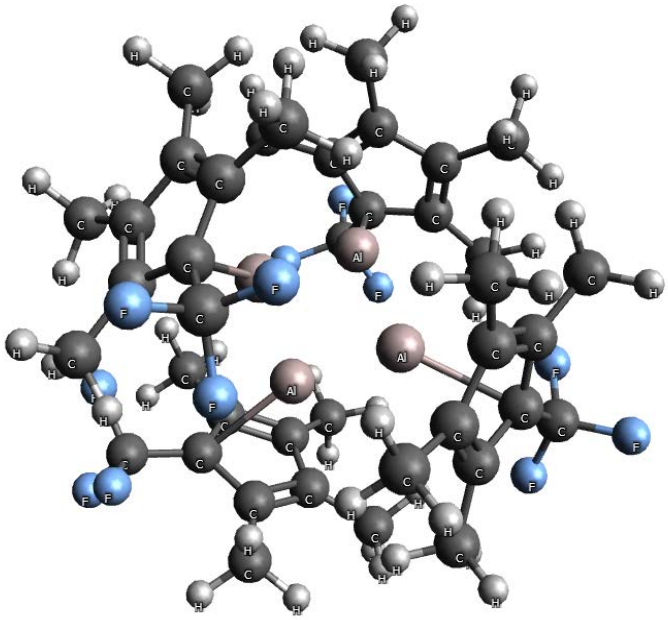

Figure 7. Tetramer $Al_4C_{40}H_{48}F_{12}$

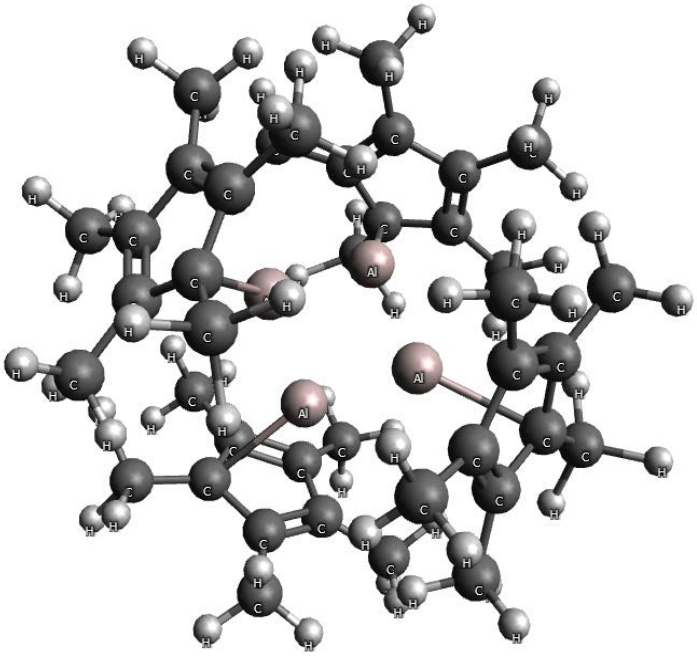

Figure 8. Tetramer $Al_4C_{40}H_{60}$

The tetramers are made up of four of each monomers respectively. This allows evaluation of the binding energy to see if the nanoclusters will form and be stable. Experimental data is available for the methylated compounds to compare with results. There is no experimental data available for the fluorine variants.

THIS PAGE INTENTIONALLY LEFT BLANK

V. RESULTS AND ANALYSIS

We next discuss key simulation results. To re-iterate, only the tetrameric methylated cluster ($Al_4C_{40}H_{60}$) has experimental data to compare with. On these systems we observe mainly the Al-Al and Al-C bond lengths and the binding energy. The binding energy is defined as

$$\Delta E_{tetra} = E_{tetra} - 4E_{mon}$$

where E_{mon} is the final energy of the monomeric molecule and E_{tetra} is the final energy of the equivalent tetramer.

First we verify the optimization results. To verify SIESTA has performed optimization correctly we observe the final atomic forces and the profile of the energy per relaxation step. The atomic forces must be close enough to zero as shown in Figure 9. Furthermore, the energy profile must show descent towards energy minimum at every step. For all systems under study, good energy optimization was obtained as depicted in Figure 10 through Figure 15. Once the energy minimum has been reached, succeeding relaxation steps show no significant energy difference.

```
siesta: Atomic forces (eV/Ang):
     1     0.004627   -0.004454   -0.004615
     .          .           .           .
     .          .           .           .
     .          .           .           .
     2     0.005806    0.013695   -0.003214
   104     0.009682   -0.007622   -0.007005
----------------------------------------
   Tot     0.011062    0.007595   -0.002929
----------------------------------------
   Max     0.032293
   Res     0.010008    sqrt( Sum f_i^2 / 3N )
----------------------------------------
   Max     0.032293    constrained
```

Figure 9. Atomic forces, good optimization

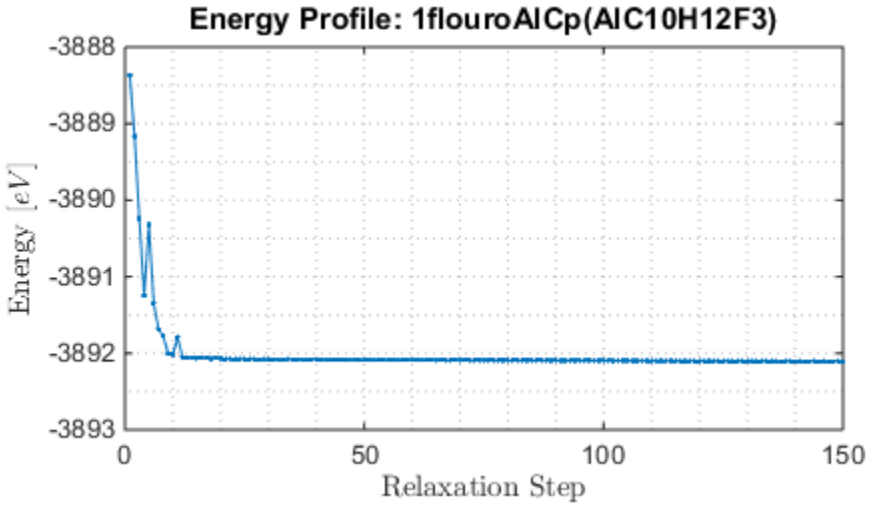

Figure 10. Energy per relaxation step for $AlC_{10}H_{12}F_3$

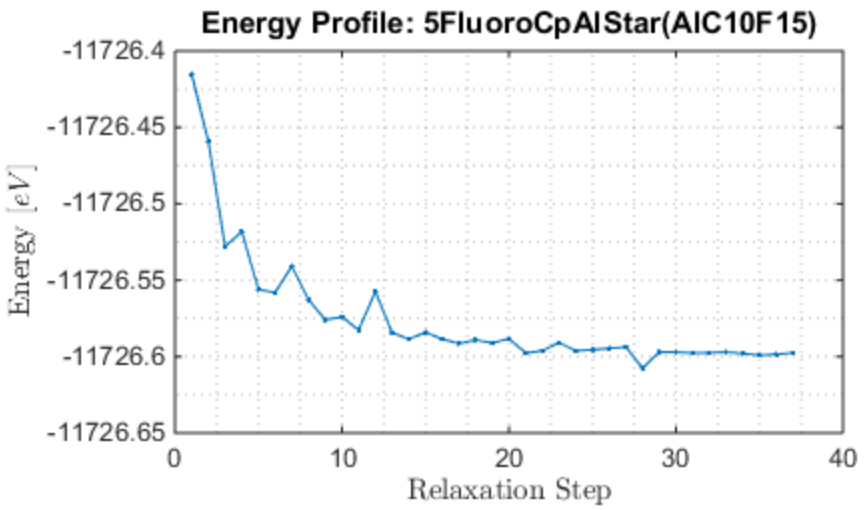

Figure 11. Energy per relaxation step for $AlC_{10}F_{15}$

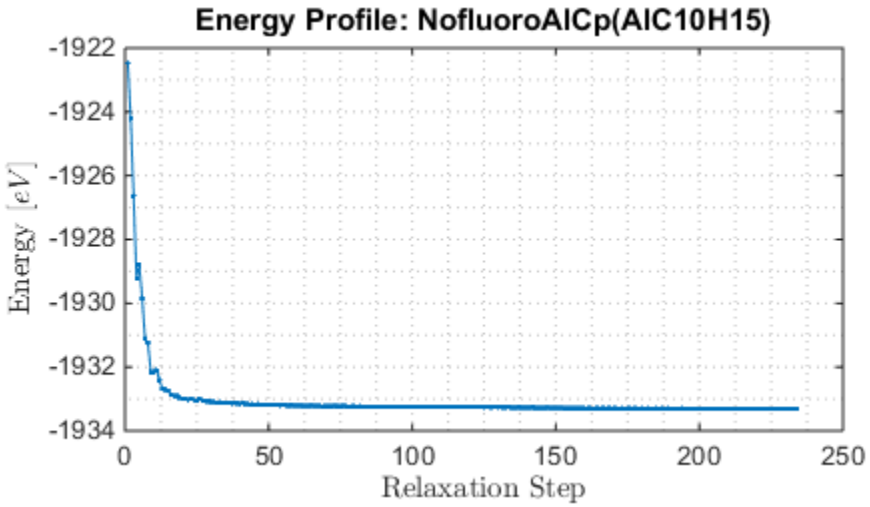

Figure 12. Energy per relaxation step for $AlC_{10}H_{15}$

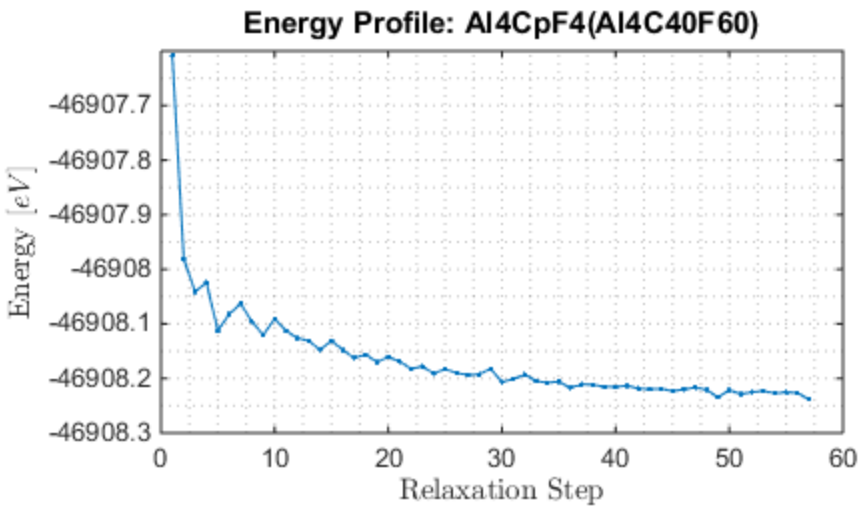

Figure 13. Energy per relaxation step for $Al_4C_{40}F_{60}$

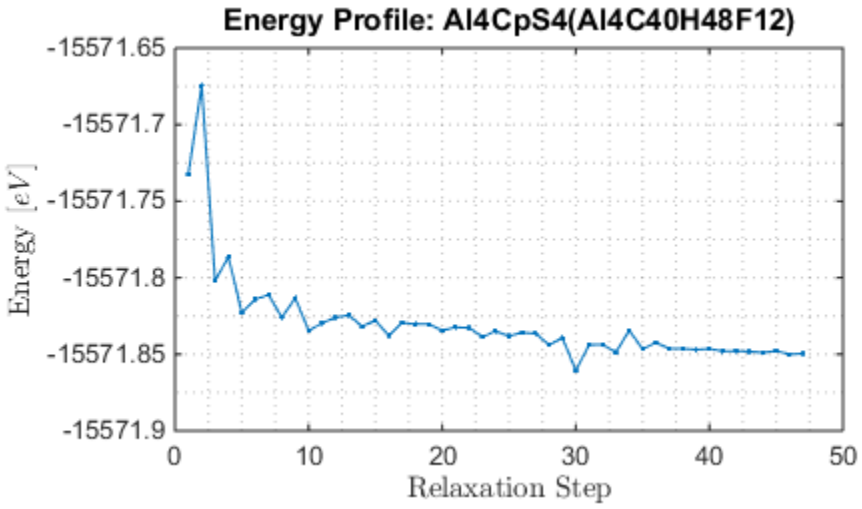

Figure 14. Energy per relaxation step for $Al_4C_{40}H_{48}F_{12}$

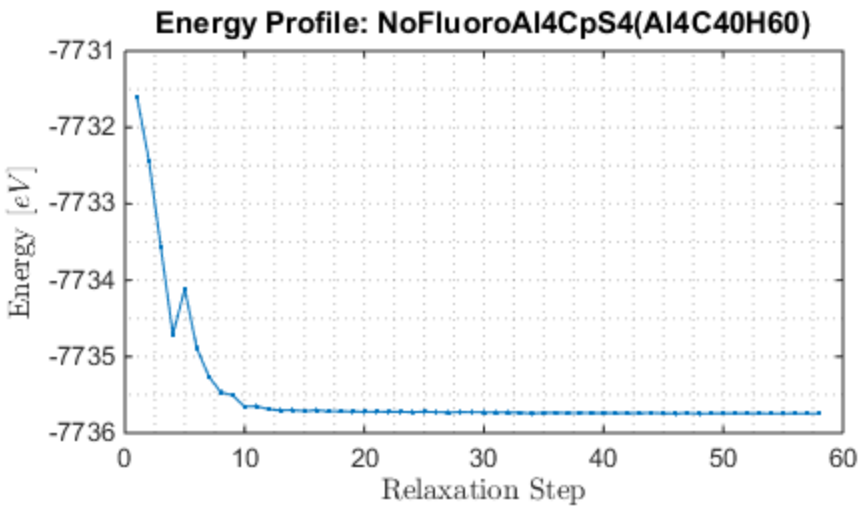

Figure 15. Energy per relaxation step for $Al_4C_{40}H_{60}$

As depicted in the Figure 10 to Figure 15, the energy minimization problem was resolved adequately. Therefore SIESTA was able to find the optimal spatial atomic coordinates for each molecule. From the graphs one can immediately note that the non-fluorine molecules tend to approach the final structure with fewer fluctuations.

The bond lengths were also measured using the Avogadro visualization program. These measurements are presented in Table 1. The experimental data arises from the article by Huber and Schnöckel [3] in which X-ray crystallography was utilized.

Table 1. Bond lengths in Angstroms (Å)

	Al-Al		Al-Cp_{centre}	
	Average(Sim)	Experimental	Average(Sim)	Experimental
$Al_4C_{40}H_{60}$	2.8142	2.767	2.0778	2.011
$Al_4C_{40}F_{60}$	2.9078	-	2.2542	-
$Al_4C_{40}H_{48}F_{12}$	2.7988	-	2.0963	-

The bond lengths obtained from the DFT simulation are not far off from the experimental measurements. Simulation Al-Al bond length is approximately 0.05Å larger. This offers confidence in the SIESTA method for the other molecules. Also this can be expected as the experiment used solid form of the cluster. For $Al_4C_{40}H_{48}F_{12}$ the Al-Al bond is weaker which implies less stability.

The projected density of states (PDOS) and the total density of states were also obtained. The PDOS shows a lot of interaction between Al and C for all molecules. This makes sense since they are bonded. The PDOS and the DOS are shown in Figure 16 through Figure 27. The Fermi energy is indicated in the graphs by a vertical line. Additional Al states in the valence of $Al_4C_{40}H_{48}F_{12}$ (Figure 23) indicate extra Al bonding. The HOMO/LUMO gap of the monomers approaches that of insulators. The HOMO/LUMO gaps of the tetramers is reduced due to metallic bonding. The partially fluorinated $Al_4C_{40}H_{48}F_{12}$ cluster is highly bonded with binding energy of -289 kJ/mol compared to that of the fully-fluorinated ($Al_4C_{40}F_{60}$) and none-fluorinated ($Al_4C_{40}H_{60}$) clusters with binding energies -178 kJ/mol and 219 kJ/mol, respectively. Binding energy is increased for the partially fluorinated group although the Al-Al bond is not closer in the structure. This could be due to the interaction between the ligands (additional binding). From the experimental data the binding energy of the fully-hydrogenated cluster was measured to be -155 kJ/mol (Table 2).

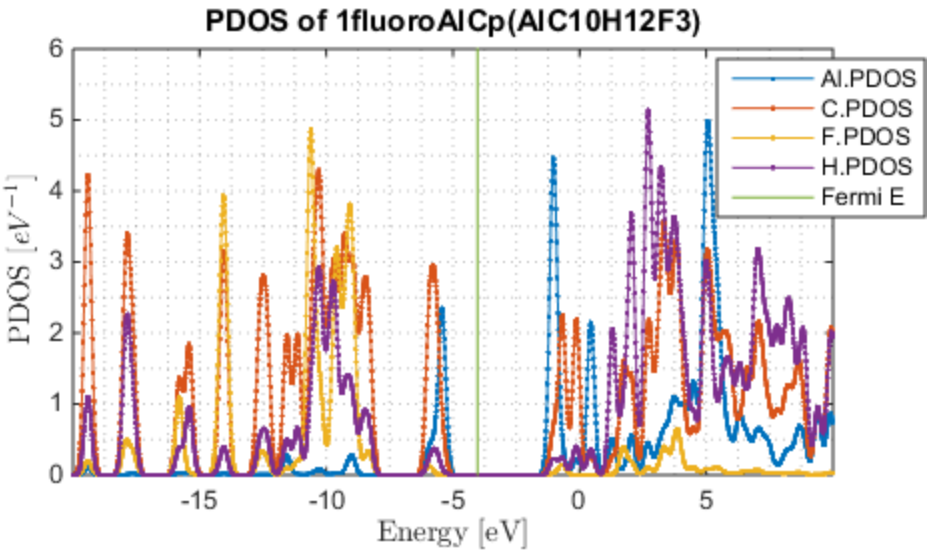

Figure 16. PDOS for $AlC_{10}H_{12}F_3$

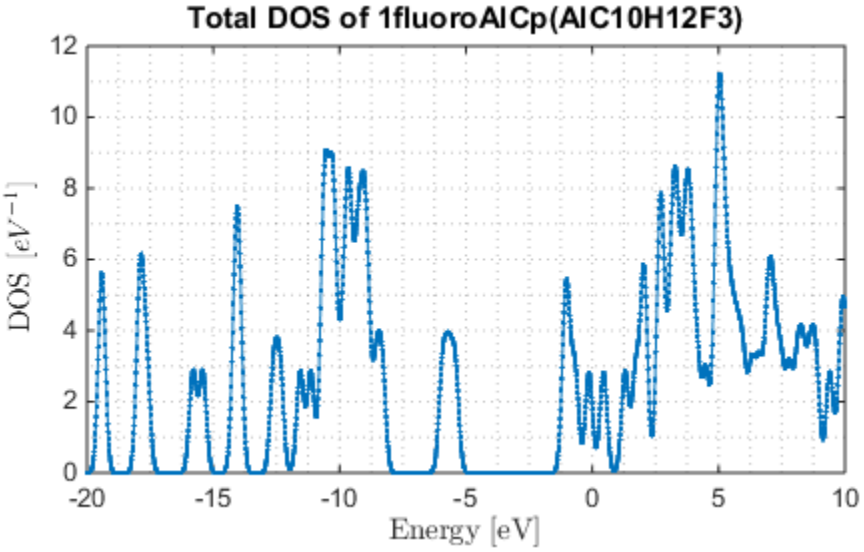

Figure 17. Total DOS for $AlC_{10}H_{12}F_3$

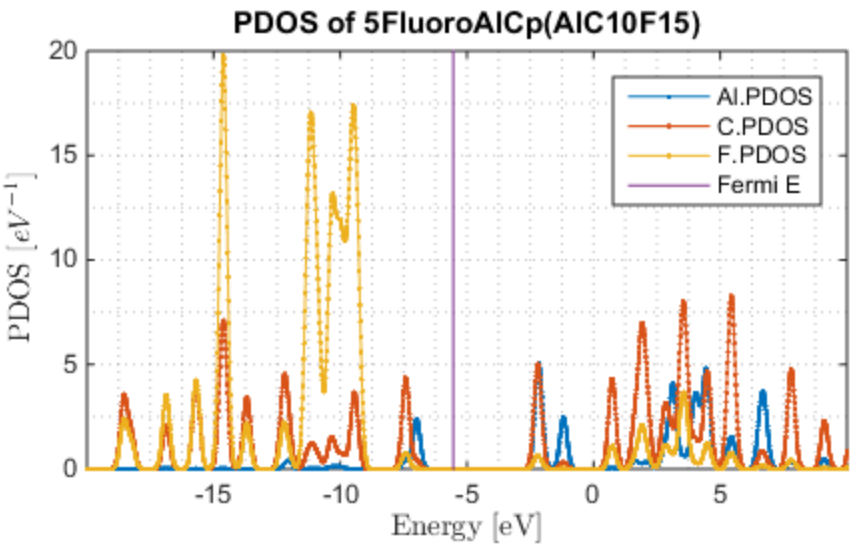

Figure 18. PDOS for $AlC_{10}F_{15}$

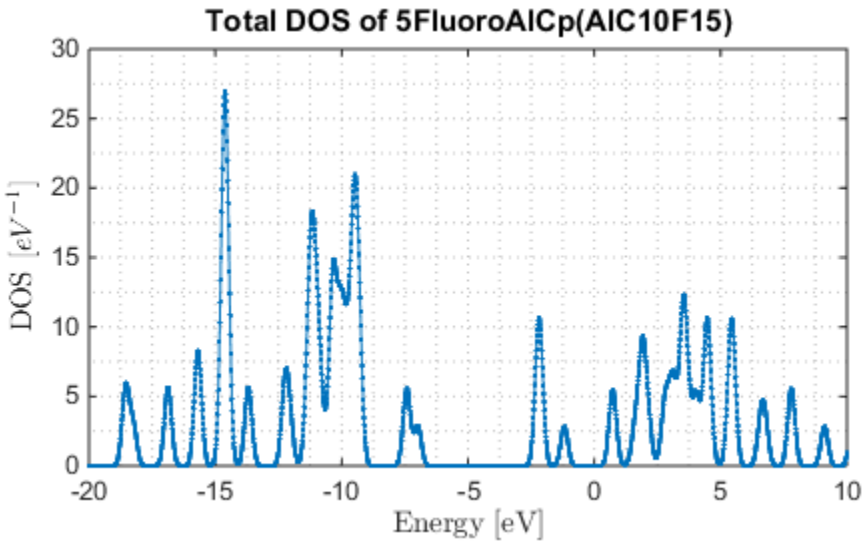

Figure 19. Total DOS for $AlC_{10}F_{15}$

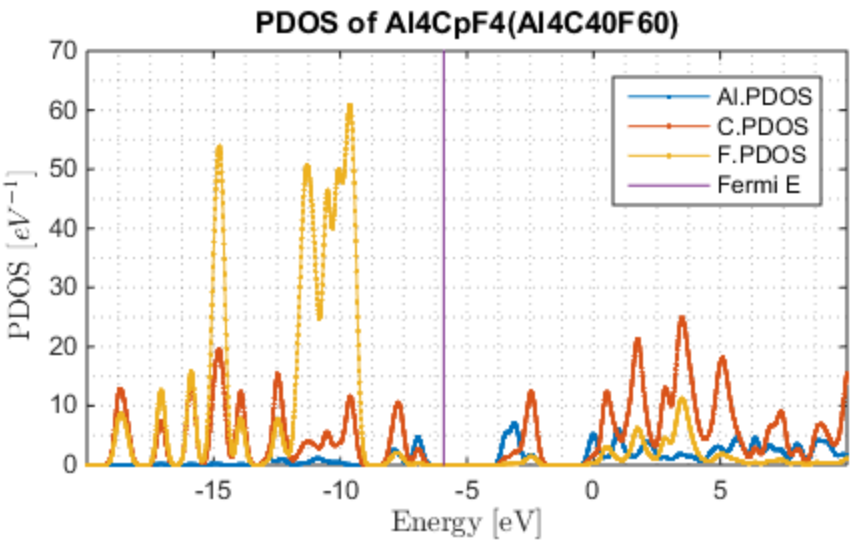

Figure 20. POS for $Al_4C_{40}H_{60}$

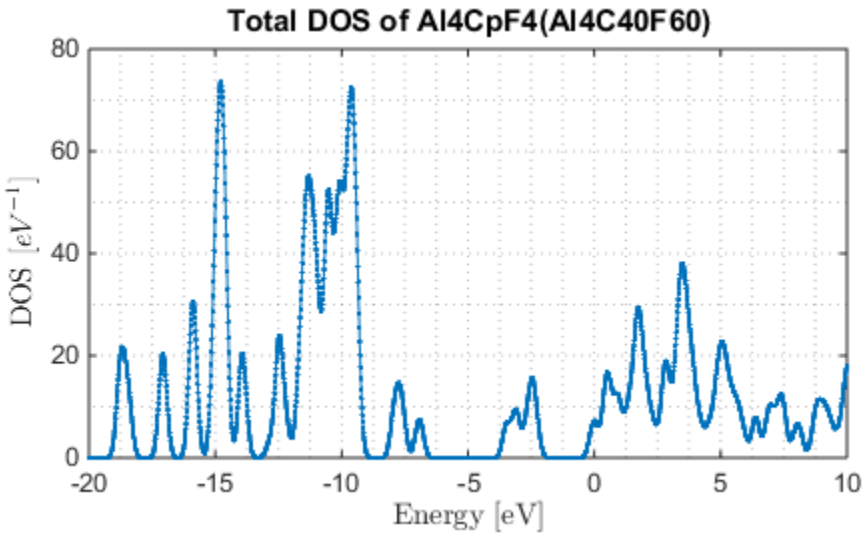

Figure 21. Total DOS for $Al_4C_{40}H_{60}$

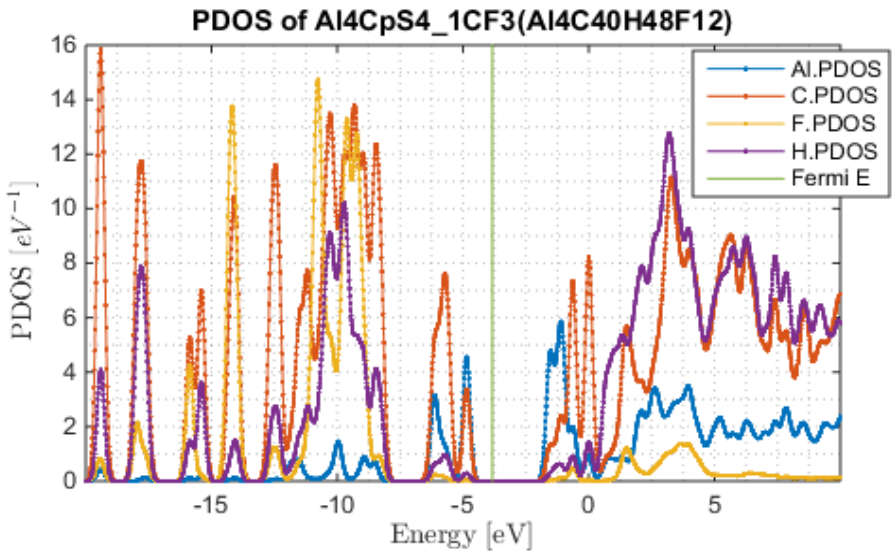

Figure 22. PDOS for $Al_4C_{40}H_{48}F_1$

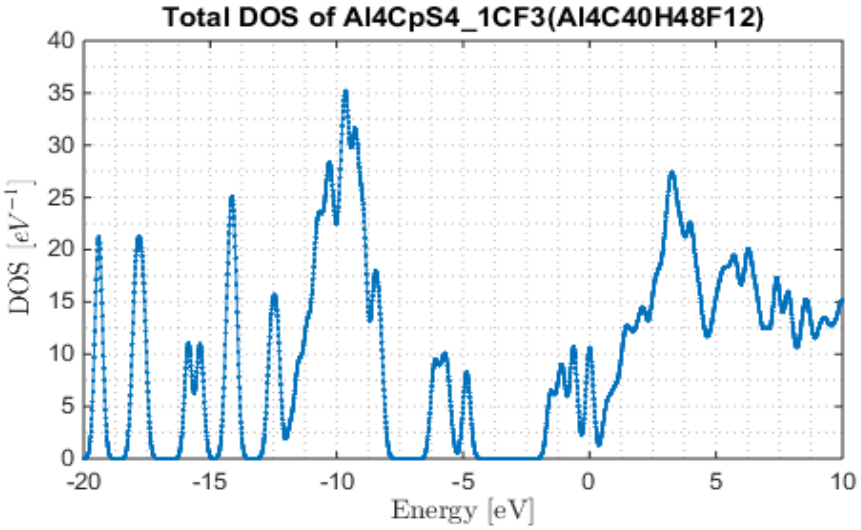

Figure 23. Total DOS for $Al_4C_{40}H_{48}F_{12}$

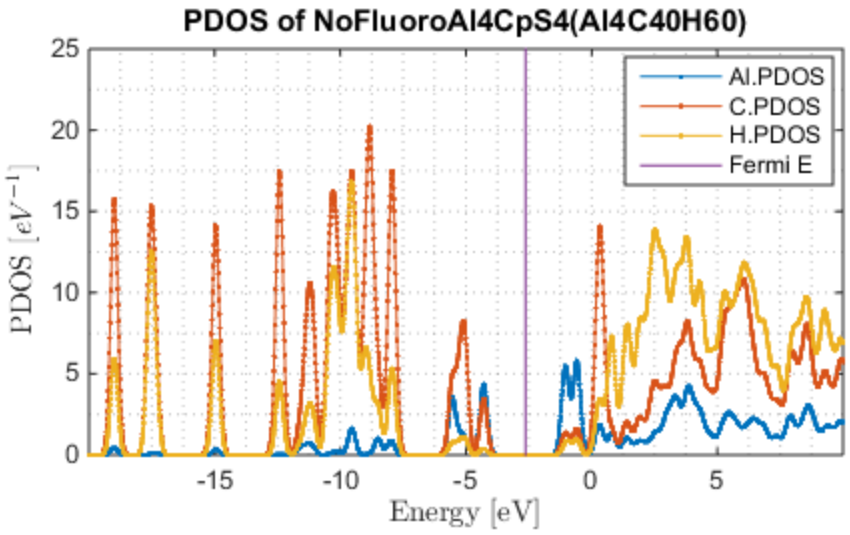

Figure 24. PDOS for $Al_4C_{40}H_{60}$

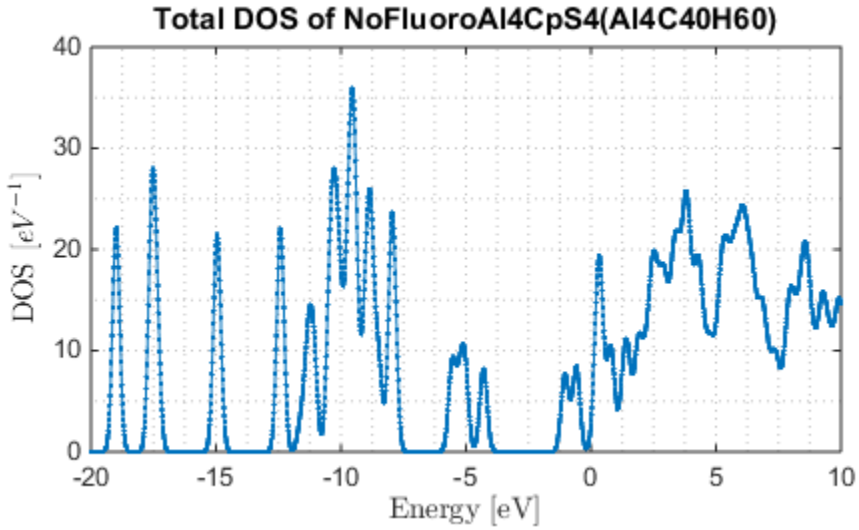

Figure 25. Total DOS for $Al_4C_{40}H_{60}$

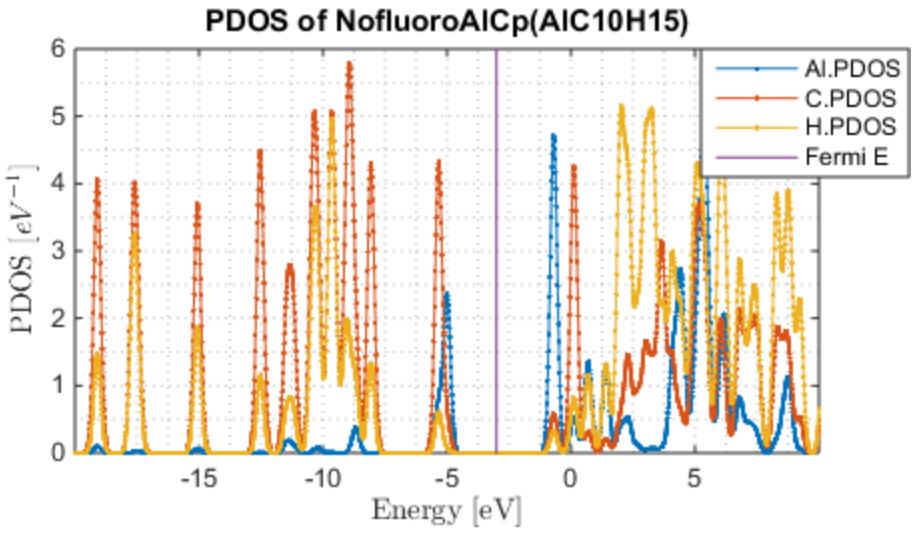

Figure 26. PDOS for $AlC_{10}H_{15}$

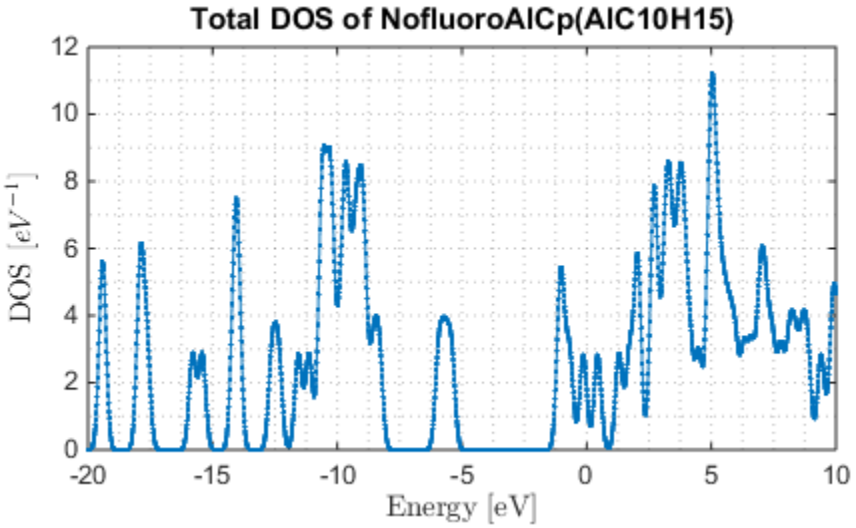

Figure 27. Total DOS for $AlC_{10}H_{15}$

Table 2. Calculated binding energy, HOMO/LUMO gap and Fermi energy

	ΔE_{tetra} [kJ/mol]		HOMO/LUMO Gap [eV]	Fermi Energy [eV]
	Simulation	Experimental		
$AlC_{10}H_{12}F_3$	-	-	3.166	-4.033
$AlC_{10}F_{15}$	-	-	3.662	-5.545
$AlC_{10}H_{15}$	-	-	3.121	-3.01
$Al_4C_{40}F_{60}$	-178	-	2.356	-5.921
$Al_4C_{40}H_{48}F_{12}$	-289	-	2.146	-3.834
$Al_4C_{40}H_{60}$	-219	-155	2.071	-2.632

Next we show molecular dynamics results. The molecular dynamics part of this study focused on the partially fluorinated and the no-fluorine clusters. The Verlet method was used in finding the best length of a time step. A 0.5 fs time step showed better total energy conservation as opposed to 1.0 fs. The total energy of the system is better conserved when MD Verlet runs with a 0.5 fs length of time step (Figure 28 and Figure 29) although the deviation is not a lot. The temperature is also stable (Figure 30 and Figure 31).

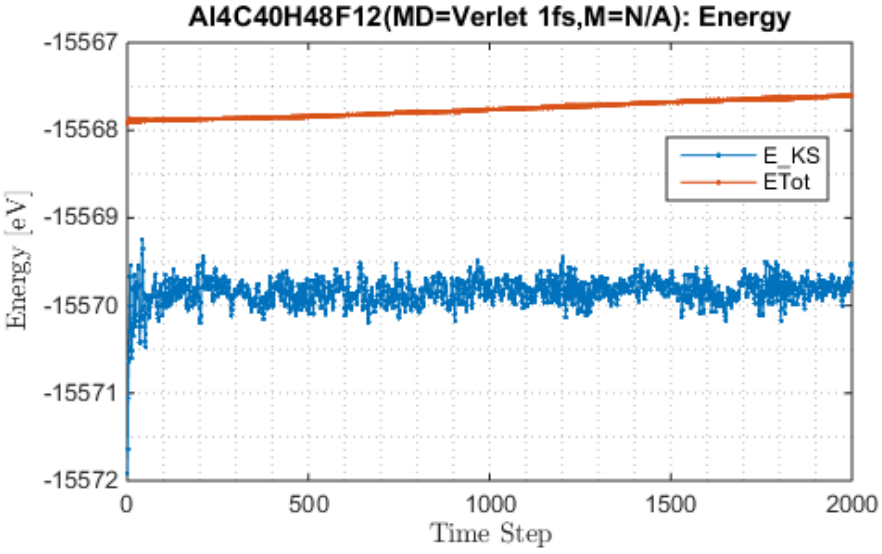

Figure 28. Total energy drifting with MD=Verlet, and length of time step at 1 fs

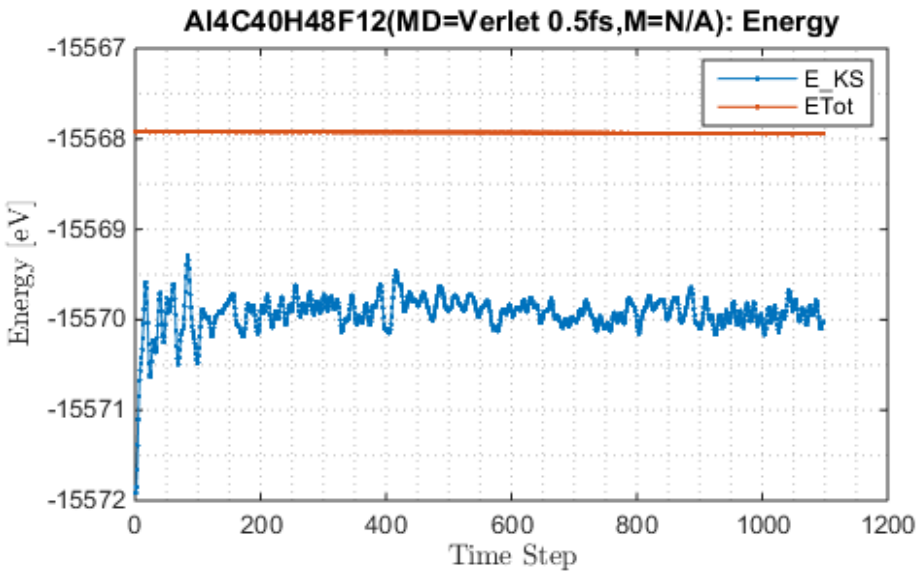

Figure 29. Total energy conserved with MD=Verlet, and length of time step at 0.5 fs

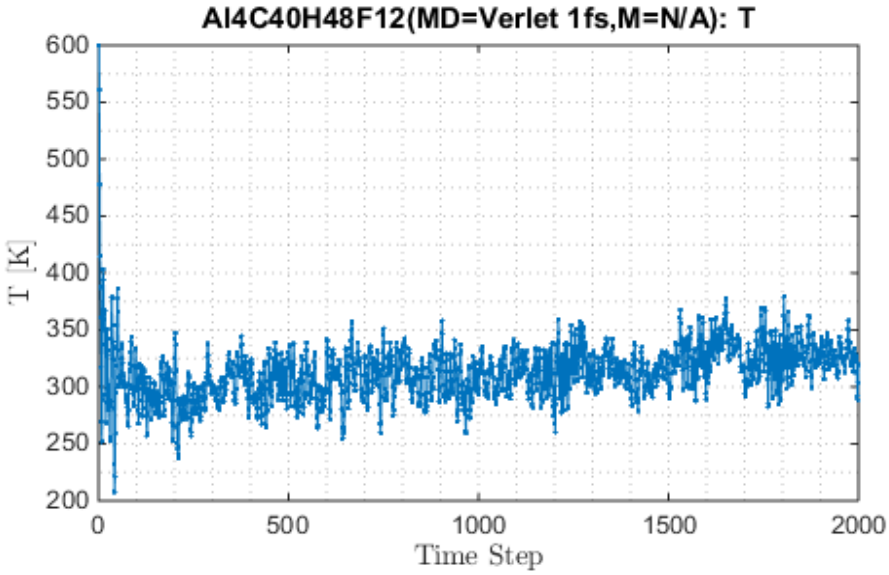

Figure 30. Temperature over time with Verlet and and length of time step at 1fs

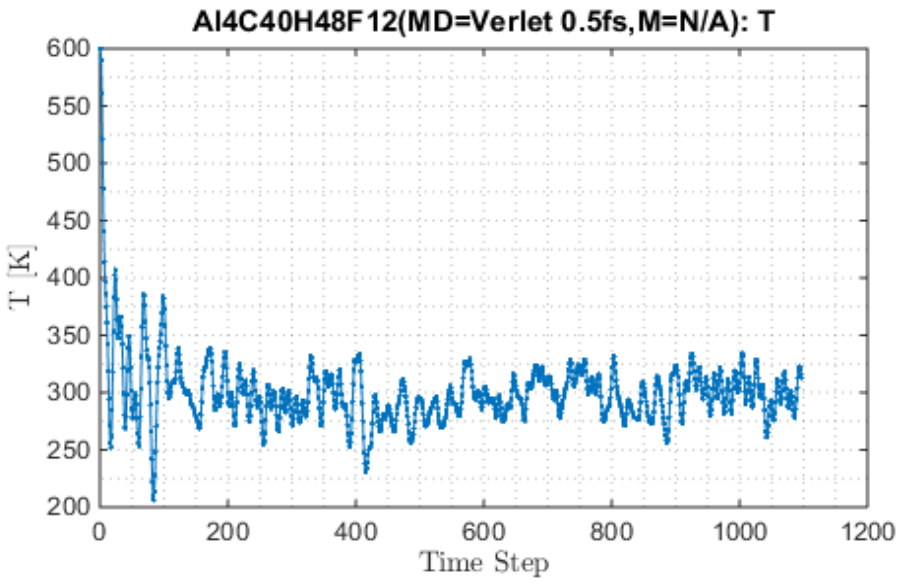

Figure 31. Temperature over time with Verlet and length of time step at 0.5 fs

For the Nose (main interest), several mass settings and length of time step were attempted. The enforced temperature for the Nose is 600K. For a default mass at 1 fs time step the energy exhibits similar characteristics as that of Verlet at 1 fs. For the setting of Nose with masses 1 and 50 either with 1 fs or 0.5 fs time step, the energy and the temperature over time exhibit dramatic fluctuations and a non-conserved energy (Figure 32 through Figure 34).

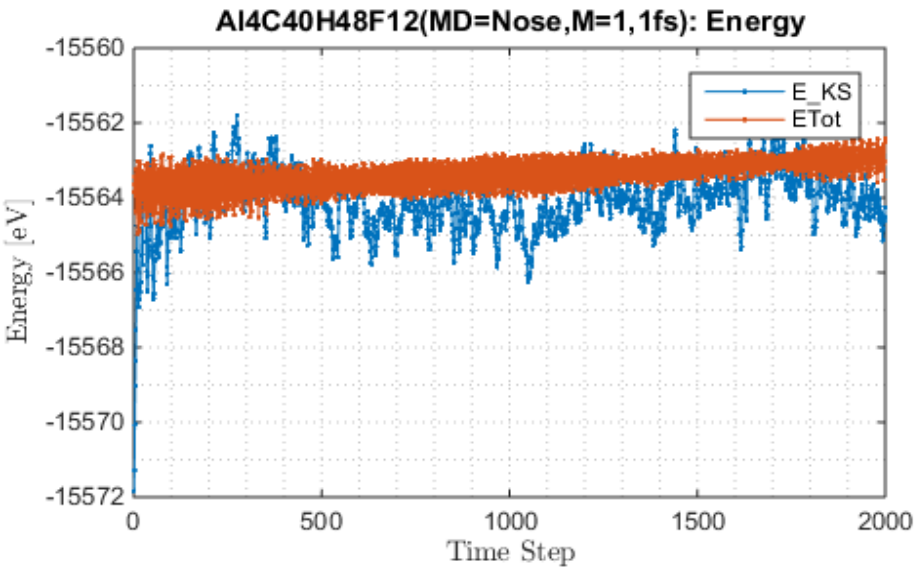

Figure 32. Energy with Nose at 1 fs and a mass of 1

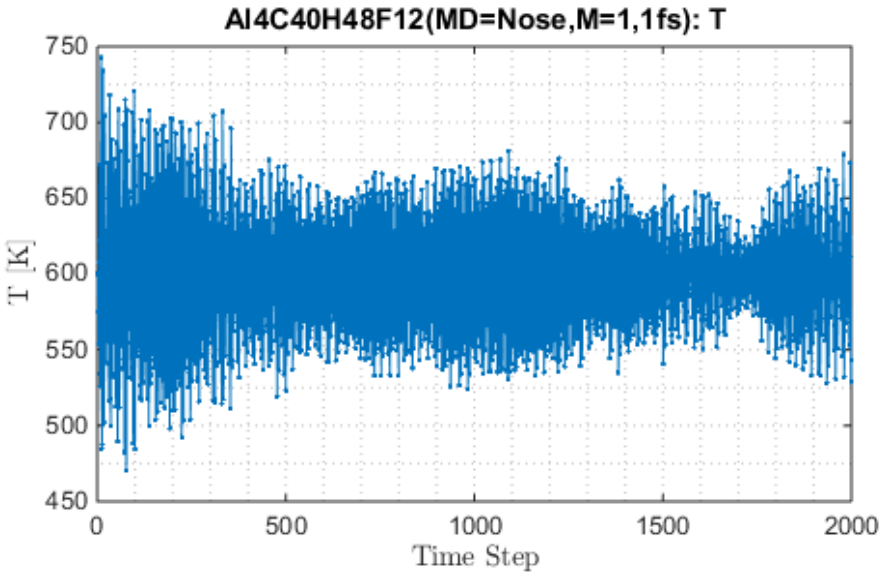

Figure 33. Temperature fluctuations over time when mass is set to 1

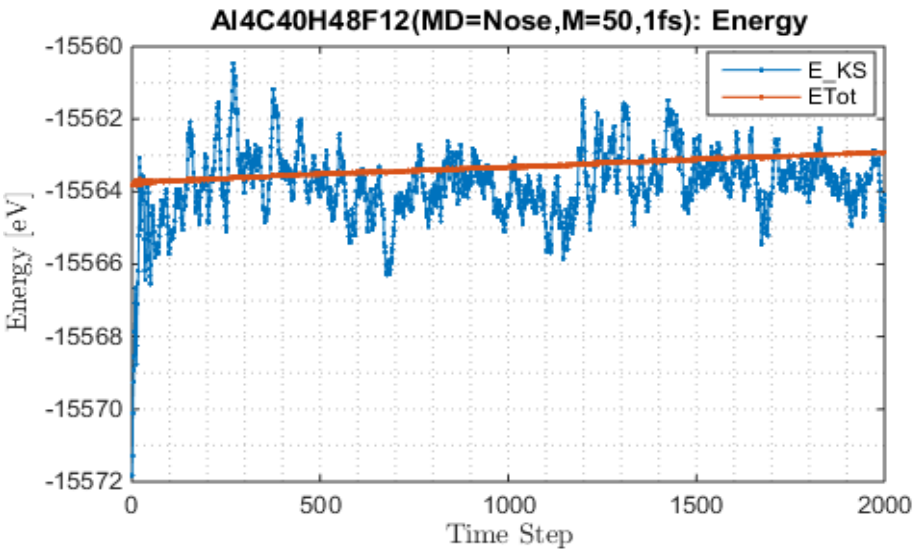

Figure 34. Total energy drifting with MD=Nose, and length of time step at 1 fs and a mass of 50

Good results are obtained when mass is set to default (M=100) and the length of time step is 0.5 fs. Although slight fluctuations in temperature are observed the energy is well conserved. The fluctuations in temperature have a standard deviation of approximately 64K. Furthermore, it was observed that these fluctuations arise from the manner in which SIESTA enforces the temperature (i.e., algorithmic). Figure 35 and Figure 36 show the results with default mass at 0.5 fs of the $Al_4C_{40}H_{48}F_{12}$ cluster. Consequently, Figure 37 and Figure 38 show the results for the $Al_4C_{40}H_{60}$ cluster. For this setup the MD simulation was allowed to run for a longer number of time steps.

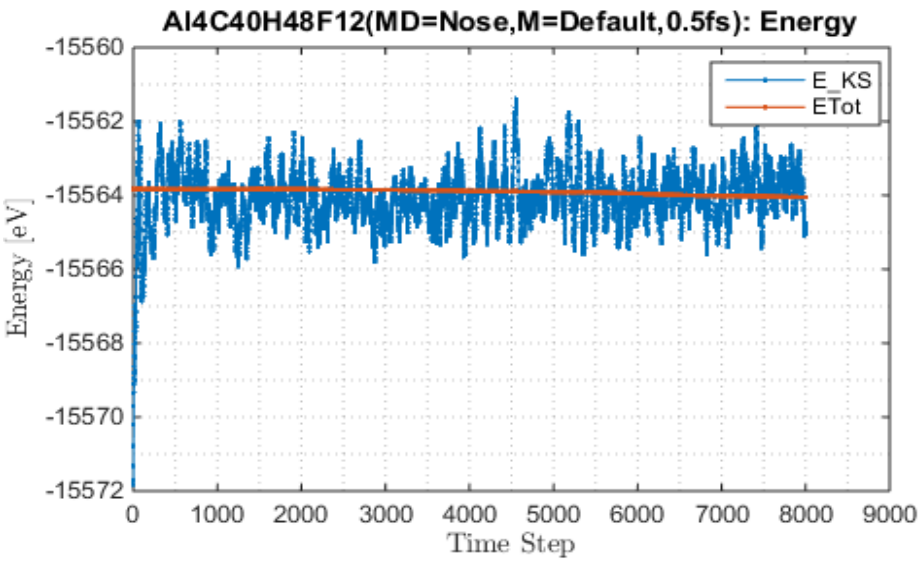

Figure 35. Energy with Nose MD at 0.5 fs and a mass of 100 for $Al_4C_{40}H_{48}F_{12}$

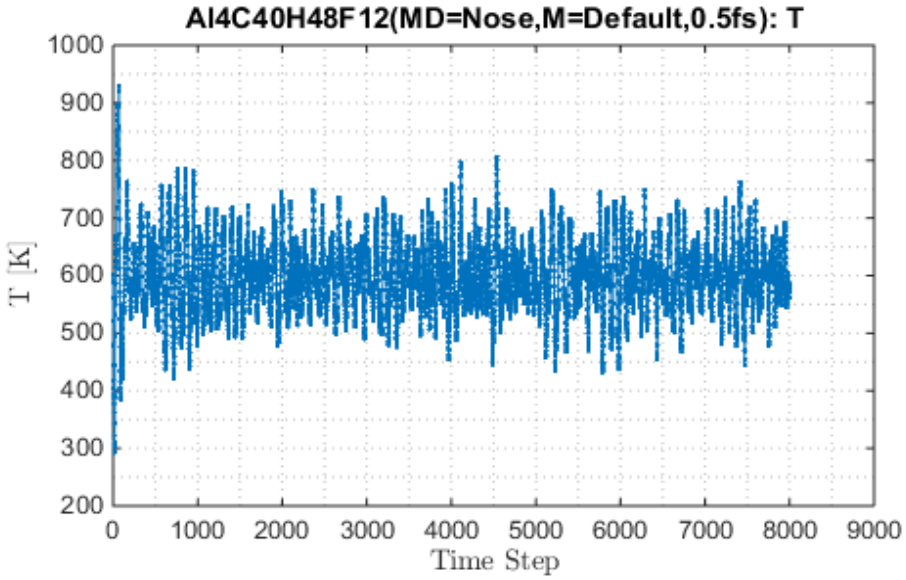

Figure 36. Temperature over time with Nose and length of time step at 0.5 fs for $Al_4C_{40}H_{48}F_{12}$

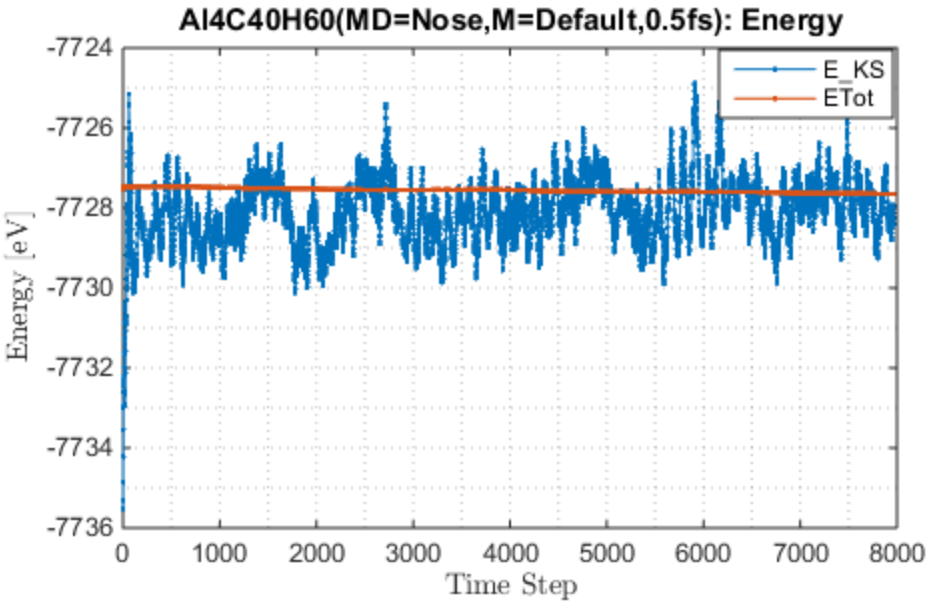

Figure 37. Energy with Nose MD at 0.5 fs and a mass of 100 for $Al_4C_{40}H_{60}$

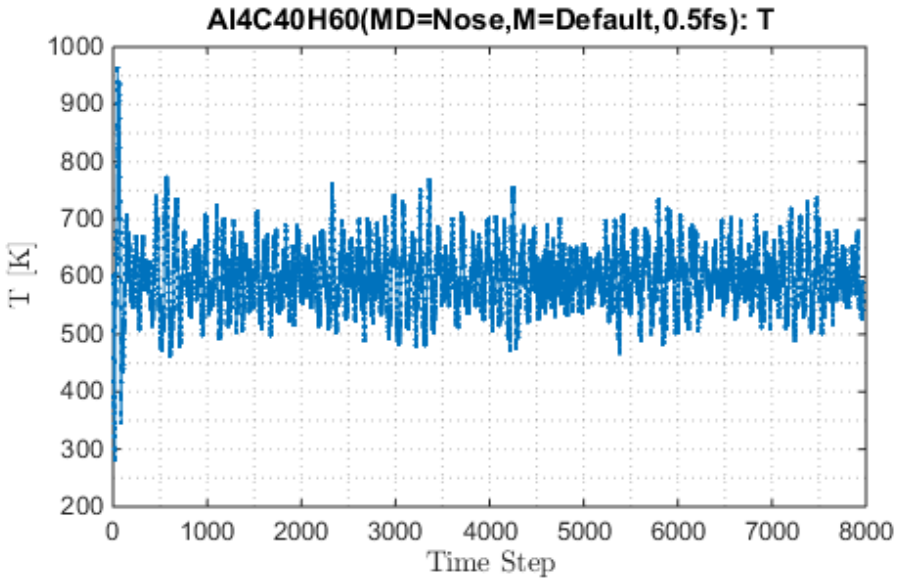

Figure 38. Temperature over time with Nose and and length of time step at 0.5 fs for $Al_4C_{40}H_{60}$

Using VMD software, the trajectory was visualized and verified that it does not break apart over time. Sample snapshots of the partially-fluorinated cluster at different time steps are shown in Figure 39 to Figure 42. As can be seen from the snapshots, the atoms' positions change only slightly, however the overall molecule remains intact.

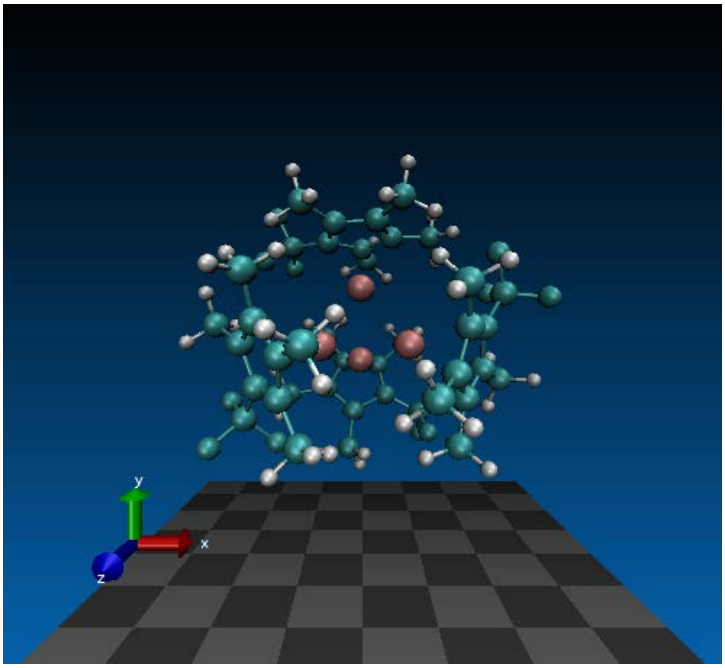

Figure 39. Snapshot of trajectory at start

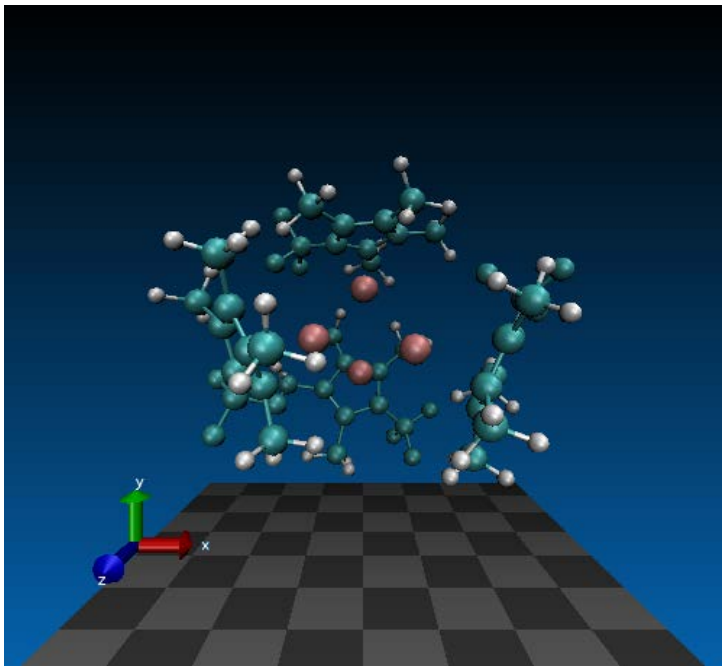

Figure 40. Snapshot of trajectory after 400 time steps

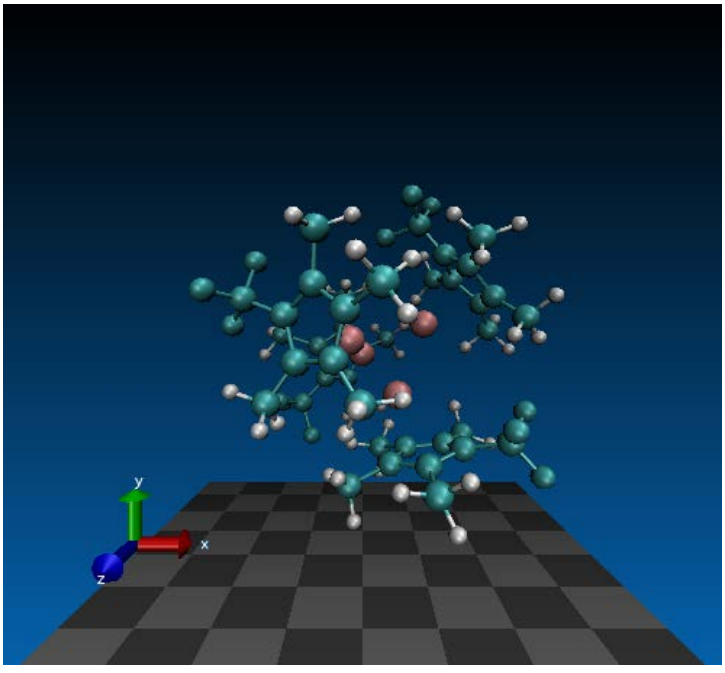

Figure 41. Snapshot of trajectory after 5000 time steps

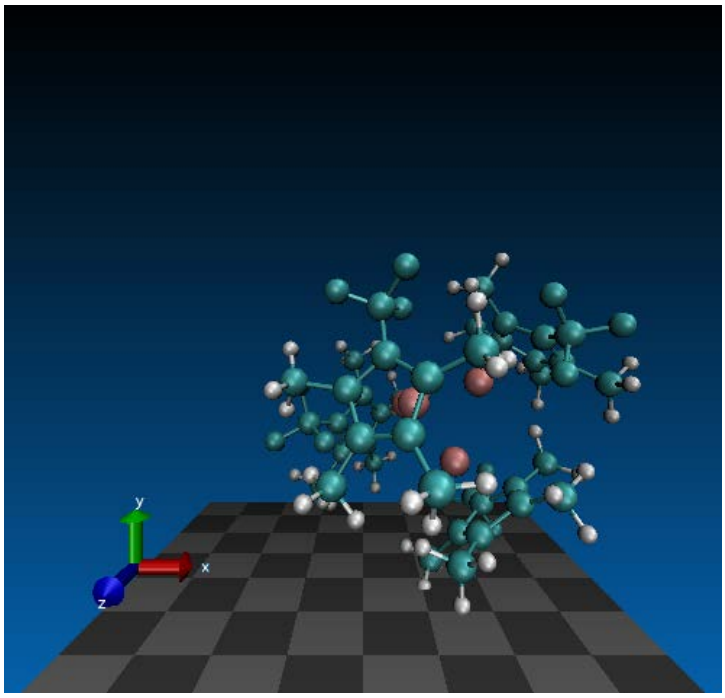

Figure 42. Snapshot of trajectory after 10566 time steps

VI. CONCLUDING REMARKS

This thesis examined three metalloid aluminum clusters along with their corresponding monomers. The SIESTA DFT code was used to simulate the properties of these molecules. Calculations were validated by comparison to the experimentally-known $Al_4C_{40}H_{60}$. For this methylated cluster the Al-Al and Al-Cp_{centre} (Al to the center of the Cp-ligand) bond lengths were within 0.05 Angstoms to the available experimental data. The bond lengths in the fully-fluorinated and partially-fluorinated clusters were found to be longer, however still fairly close to that of the methylated cluster. The partially fluorinated cluster ($Al_4C_{40}H_{48}F_{12}$) was found to have the highest binding energy (-289 kJ/mol). The $Al_4C_{40}F_{60}$ and the $Al_4C_{40}H_{60}$ are also considered strongly binded, -178 kJ/mol and -219 kJ/mol, respectively. This particular simulation method overpredicted the $Al_4C_{40}H_{60}$ binding compared to experimental data; this energy is known to be very sensitive to the functional used. We expect that relative changes in the binding energy are still accurate, and that the replacement of a single methyl group in each Cp^* results in a stronger binding energy. The Al-Al distance does not differ significantly from $Al_4C_{40}H_{60}$, suggesting that the increased binding is due to weak non-covalent interactions within the ligands. By visual inspection of the MD results the structures were stable even when subjected to simulated temperatures of 600 K.

The next step in investigating these Al_4 clusters will be to predict their crystal structure by integrating the SIESTA results into a program such as USPEX. This will enable further interrogation of the suitability of these Al_4Cp_4 compounds in explosives.

THIS PAGE INTENTIONALLY LEFT BLANK

LIST OF REFERENCES

[1] M. Mandado, A. Krishtal, C. Van Alsenoy, P. Bultinck, and J. M. Hermida-Ramón, "Bonding study in all-metal clusters containing Al_4 units," *J. Phys. Chem. A*, Vol. 111, No. 46, pp. 11885–11893, 2007.

[2] K. S. Williams and J. P. Hooper, "Structure, thermodynamics, and energy content of Aluminum-Cyclopentadienyl clusters", *J. Phys. Chem*. A, Vol. 115, No. 48, pp. 14100–14109, Dec. 2011.

[3] M. Huber and H. Schnöckel, "$Al_4(C_5Me_4H)_4$: structure, reactivity and bonding", *Inorganica Chemica Acta,* Vol. 361, pp. 457–461, April 2007.

[4] T Watanabe, K Koyasu, and T Tsukuda, "Density functional theory study on stabilization of the Al_{13} Superatom by Poly(vinylpyrrolidone)," *J. Phys. Chem. C*, Vol. 119, No. 20, pp. 10904−10909, May 2015.

[5] N. G. Karpukhina, U. Werner-Zwanziger, J. W. Zwanziger, and A. A. Kiprianov, "Preferential binding of Fluorine to Aluminium in high Peralkaline Aluminosilicate glasses," *J. Phys. Chem. B*, Vol. 111, No. 35, pp. 10413–10420, Sept. 2007.

[6] A. Mañanes, F. Duque, F. Me´ndez, M. J. Lo´pez and J. A. Alonso, "Analysis of the bonding and reactivity of H and the Al_{13} cluster using density functional concepts," *J. Chem. Phys.*, Vol. 119, No. 10, Sept. 2003.

[7] E. Artacho, E. Anglada, O. Dieguez, J. D. Gale, A. Garcia, J. Junquera, R. M. Martin, P. Ordejon, J. M. Pruneda, D. Sanchez-Portal and J. M. Soler, "The SIESTA method; developments and applicability," *J. Phys. Condens. Matter*, Vol. 20, No. 6, pp. 064208, 2008.

[8] *The SIESTA Manual*, Siesta 4.1-b1, The Siesta Group, http://www.uam.es/siesta, 2016.

[9] Density functional theory [Online], Accessed: 04 Nov. 2016, Available: https://en.wikipedia.org/wiki/Density_functional_theory

[10] A. Marthinsen. (2016, Jan 28). Fundamentals and applications of density functional theory [Online]. Available: www.virtualsimlab.com/s/VSL-talk.pdf

[11] E. Artacho. (2014, Sept.) Molecular dynamics: Theory [Online]. Available: http://departments.icmab.es/leem/siesta/tlv14/

THIS PAGE INTENTIONALLY LEFT BLANK

APPENDIX A. THE FDF FILE

```
SystemName          falc
SystemLabel         1FAlCpMethFull

NumberOfAtoms       26

NumberOfSpecies     4
%block ChemicalSpeciesLabel
    1   6  C
    2   1  H
    3   9  F
    4   13 Al
%endblock ChemicalSpeciesLabel

AtomicCoordinatesFormat    Ang
%block AtomicCoordinatesAndAtomicSpecies
1.34100    -2.3730    -0.1430    1
-1.8400    -2.0050    -0.2230    1
-2.4800    1.12600    -0.0090    1
0.30400    2.70900    -0.2740    1
2.67700    0.54700    -0.0600    1
0.60800    -1.0460    -0.1130    1
1.18900    0.25600    -0.1150    1
0.13100    1.20900    -0.1360    1
-1.1040    0.49700    -0.1040    1
-0.8080    -0.8960    -0.1370    1
-2.7590    -1.7220    -1.1650    2
-1.2940    -3.1840    -0.5570    2
-2.4820    -2.1820    0.95300    2
-2.8560    1.69800    -1.1630    3
-2.5010    2.07200    0.96000    3
-3.4220    0.22800    0.33000    3
1.08700    2.99600    -1.3310    2
-0.8620    3.34000    -0.4810    2
0.86500    3.25200    0.82800    2
2.94600    1.86100    -0.0470    2
3.31900    0.01100    -1.1110    2
3.22100    0.03800    1.07200    2
2.66000    -2.2390    0.06800    2
1.18800    -2.9860    -1.3290    2
0.87700    -3.1990    0.82400    2
0.00100    -0.0020    2.09500    4
%endblock AtomicCoordinatesAndAtomicSpecies

##################BasisSetParameter#################################
######
xc.functional         GGA     # Exchange-correlation functional
xc.authors            PBE     # Exchange-correlation version
```

```
LongOutput            .true.
MeshCutoff            360 Ry  # Mesh cutoff. real space mesh
MaxSCFIterations      500     # Maximum number of SCF iter
DM.MixingWeight       0.01    # New DM amount for next SCF cycle
DM.Tolerance          1.d-3
DM.NumberPulay        10
DM.MixSCF1            T

PAO.BasisType         split
PAO.BasisSize         DZP
PAO.EnergyShift       0.1 eV
PAO.SplitNorm         0.20    # between input and output DM
SolutionMethod        Diagon  # OrderN or Diagon
ElectronicTemperature 300 K   # Temp. for Fermi smearing
MD.TypeOfRun          CG      # Type of dynamics:
#MD.VariableCell      .true.  # Relaxation
MD.NumCGsteps         500     # No. of iterations in relaxation
MD.MaxForceTol        0.04 eV/Ang # Force Tolerance

%block PDOS.KgridMonkhorstPack
    15   0    0    0.0
    0    15   0    0.0
    0    0    15    0.0
%endblock PDOS.KgridMonkhorstPack

%block ProjectedDensityOfStates
-20.00 10.00 0.2 2000 eV
%endblock ProjectedDensityOfStates


COOP.Write T

WriteCoorInitial        .true.
WriteForces             .true.
WriteEigenvalues        .true.
WriteMullikenPop        1
WriteWaveFunctions      .true.
UseSaveData             .true.
DM.UseSaveDM            .true.
MD.UseSaveXV            .true.
MD.UseSaveCG            .true.
SaveRho                 .true.
SaveDeltaRho            .true.
WriteSiestaDim          .true.
WriteDenchar            .true.
WriteCoorStep           .true.
```

APPENDIX B. SLURM CODE SNIPPET

```
#!/bin/bash
#SBATCH --nodes=1
#SBATCH --ntasks-per-node=64
#SBATCH --mem-per-cpu=400M
#SBATCH --time=72:00:00
#SBATCH --job-name=LiGr_02
#SBATCH --account=MyProjectName
#####SBATCH --export=NONE

source /etc/profile
cd $SLURM_SUBMIT_DIR

module load compile/intel/17.0 mpi/openmpi/2.0.1

mpirun    -np    64    /work/smalnemr/siesta-3.1.t/Obj/siesta    <
Cluster.fdf | tee test_opt_1fluoroAlCp.out
```

THIS PAGE INTENTIONALLY LEFT BLANK

INITIAL DISTRIBUTION LIST

1. Defense Technical Information Center
   Ft. Belvoir, Virginia

2. Dudley Knox Library
   Naval Postgraduate School
   Monterey, California